GENERAL SYMPOSIA | INJECTION MOLDING

Material Selection for Injection Molding Hollow Microneedles

Tim Evens, Pol Vanwersch, Sylvie Castagne and Albert Van Bael

DOI: https://doi.org/10.51573/Andes.PPS39.GS.IM.4

December 2024

Material Selection for Injection Molding Hollow Microneedles

Tim Evens, Pol Vanwersch, Sylvie Castagne and Albert Van Bael[1]

Abstract: Hollow microneedles are designed to perform intradermal medical substance delivery or fluid extraction, with polymers standing out as cost-effective materials for mass production via injection molding. However, existing research lacks a comparative analysis of different polymers in terms of processability and performance in skin penetration tests. This study addresses this gap by evaluating hollow microneedles fabricated from five biocompatible thermoplastic materials: polycarbonate (PC), polybutylene terephthalate (PBT), polylactic acid (PLA), polyamide 12 (PA12), and glass-fiber reinforced polyarylamide (PARA). Significant differences in replication fidelity were found among the thermoplastics, with a higher calculated solidification time resulting in better replication fidelity due to extended deformability during the packing phase. PBT microneedles deformed during demolding and were excluded from penetration tests. Penetration tests on piglet ears showed no penetration for PA12 and PLA microneedles due to deformation of the needles. PARA demonstrated consistent penetration results, while PC exhibited an inconsistent penetration behavior, with some needles successfully penetrating while others deformed. High mechanical properties were found to be critical for achieving consistent and successful penetration.

Keywords: Hollow Microneedles, Injection Molding, Material Selectionv

1 The authors Tim Evens (tim.evens@kuleuven.be), Pol Vanwersch (pol.vanwersch@kuleuven.be), and Albert Van Bael (albert.vanbael@kuleuven.be) are affiliated with the Department of Materials Engineering at the KU Leuven University in Belgium. Sylvie Castagne (sylvie.castange@kuleuven.be) and Pol Vanwersch are also affiliated with the Department of Mechanical Engineering and Flanders Make@KU Leuven at the same university.

DOI: https://doi.org/10.51573/Andes.PPS39.GS.IM.4

Introduction

Hollow microneedles are miniature needle-like structures designed to perform intradermal medical substance delivery or fluid extraction [1]. Over the years, various types of materials, including silicon, metals, ceramics, and polymers have been reported in literature for manufacturing microneedles [2]. Polymers particularly stand out as an excellent material for microneedles, as they can be cost-effective for mass production through injection molding [3]. While several polymers have been proposed in literature for microneedle fabrication, there is a notable absence of studies comparing their processability and performance during skin penetration tests. Existing research tends to highlight individual polymers, emphasizing their advantages without providing a systematic exploration of differences among various candidates.

This study addresses this gap by conducting a comprehensive analysis of hollow microneedles fabricated from five biocompatible thermoplastic materials: polycarbonate, polybutylene terephthalate, polylactic acid, polyamide 12, and glass-fiber reinforced polyarylamide. First, each material is assessed for its injection molding characteristics and replication fidelity. Secondly, the penetration behavior, an essential aspect of microneedle functionality, is tested through penetration tests on piglet ears.

Materials and Methods

Materials

The selected mold material is a low corrosion tool steel AISI 420, which is a common mold material within polymer injection molding. Five biocompatible thermoplastic materials were selected for this study: polyamide 12 (PA12, Vestamid Care ML67, Evonik), polycarbonate (PC, Lexan HPX8R, SABIC), polybutylene terephthalate (PBT, Valox HC325HP, SABIC), polylactic acid (PLA, MedEco ICB, BioVox), and 50% glass-fiber reinforced polyacrylamide (PARA, Ixef HC1022, Syensqo). Table 1 presents material properties of the thermoplastics, sourced from the suppliers and the material databases of Autodesk Moldflow 2023 and Moldex3D 2023.

Table 1. Material properties of the thermoplastics, sourced from the material suppliers and the material databases of Autodesk Moldflow 2023 and Moldex3D 2023.

	PA12	PC	PBT	PLA	PARA
Density (kg/m³)	1033	1100	1316	1240	1622
Young's Modulus (MPa)	1080	2400	2550	3450	19500
Tensile strength (MPa)	41	59	60	65	280
Thermal conductivity (W/m °C)	0.235	0.185	0.146	0.225	0.300
Specific heat (J/g °C)	2098	1128	1259	1167	1766
No-flow temperature (°C)	150	167	200	92	190

DOI: https://doi.org/10.51573/Andes.PPS39.GS.IM.4

Representation of the Process Chain

The process chain for manufacturing and testing hollow polymer microneedles developed by Evens et al. is illustrated in Figure 1 [4]. First, a micromachining system with a laser source ablates hollow microneedle cavities into a mold insert. The insert is then positioned within the mold housing. During the injection molding process, the polymer melt is forced into the laser-ablated cavities, forming the microneedles. Finally, the functionality of the microneedles is evaluated through skin penetration experiments.

Injection Molding

The injection molded part selected for this study is a 60×55×1.5 mm flat plate, featuring 6 different microneedles arranged in a 2×2 array. By design, these microneedles vary in shape and dimensions, with lengths ranging from 1000 µm to 1700 µm. They are centrally positioned on the plate, located 3 mm from the edge opposite to the gate. The polymer is injected through a hot runner positioned 17 mm from the edge of the plate. The mold insert corresponding to this product was designed and manufactured in a previous study [5]. Injection molding is done on an Engel ES 200/35 HL injection molding machine. The injection molding parameters for each thermoplastic are given in Table 2 and are defined to achieve a high replication fidelity. The geometry of the replicated thermoplastic microneedles is assessed using a Keyence VH-S30 digital microscope.

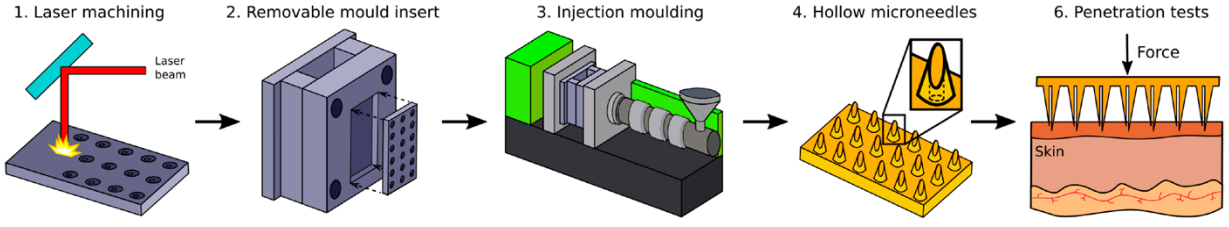

Figure 1. Illustration of the process chain to produce and test hollow polymer microneedles.

Table 2. Process parameters for injection molding.

	PA12	PC	PBT	PLA	PARA
Barrel temperature (°C)	195	310	270	210	290
Volumetric injection rate (cm^3/s)	150	150	150	150	150
Holding pressure (MPa)	95	71	95	71	95
Mold temperature (°C)	145	110	165	60	170

DOI: https://doi.org/10.51573/Andes.PPS39.GS.IM.4

The geometry of the replicated thermoplastic microneedles is assessed using a Keyence VH-S30 digital microscope. Six injection molded samples are collected and six microneedles are measured on each sample. The average of these measurements along with the standard deviation is reported in the results.

Penetration Tests

The penetration tests are designed to gain insights into the mechanisms of skin piercing and to compare the microneedles to each other in different thermoplastics. A piglet ear is used as a skin model due to its similitude to human skin [6]. For the penetration tests, a motorized tension and compression tester (BZ2.5/TS1S, Zwick) equipped with a 500-N load cell is used. For each thermoplastic, the skin penetration tests were conducted using needle type 5, the sharpest needle, (as shown in Figure 2). Each test was repeated three times using a new, unused needle. The penetration testing procedure involves placing a piglet ear beneath a downward-facing microneedle. The needle is slowly lowered towards the skin at 1 mm per minute until contact, identified by a 0.01 N threshold force. Upon contact, the needle is descended into the skin at 2 mm per minute while recording force and displacement at a rate of 1 MHz. A penetration event is defined by a sudden decrease in force, as described in [5].

Results and Discussion

Microneedle Replication Through Injection Molding

Figure 2 shows microscopic images of the six different microneedles replicated in five different thermoplastics. A clear difference in geometry can be observed among the various types of microneedles. Additionally, there is a noticeable variation in replication fidelity between the different thermoplastics, which will be further discussed in the following section. During the injection molding experiments, deformation of PBT microneedles could be observed during demolding. An example of this is Needle 2 in Figure 2. This deformation is not due to insufficient solidification, as increasing the cooling time significantly did not resolve the issue. Therefore, PBT has been excluded from the penetration experiments. Furthermore, since the PARA compound is glass-fiber reinforced grade, fibers can be seen protruding from the needles. As these fibers might cause complications if they break off in the skin during penetration, they should therefore be the subject of further analysis.

DOI: https://doi.org/10.51573/Andes.PPS39.GS.IM.4

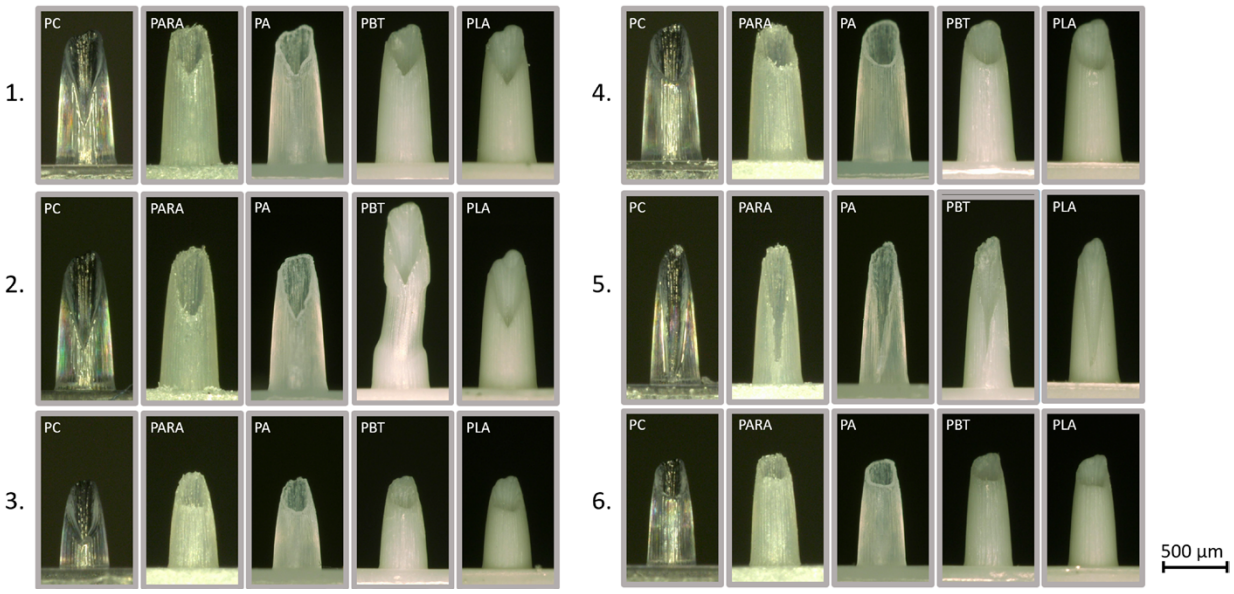

Figure 2. Microscopic images of the six different microneedles replicated in the different thermoplastics.

Figure 3 shows the average replication fidelity of the needle length and ridge height (the vertical dimension of the surrounding ridge structure) for each of the thermoplastics, alongside a micro computed tomography slice of a hollow microneedle cavity. Difference in replication fidelity between the needle length and ridge height are evident across all thermoplastics. This difference in replication fidelity is caused by the fact that the aspect ratio of the ridge-forming trench (forming the ridge height) is higher than that of the main needle cavity. This increased surface/volume ratio leads to faster freezing of the polymer and thus a lower replication fidelity. A similar relationship between aspect ratio and replication fidelity was noted by Evens et al. [7].

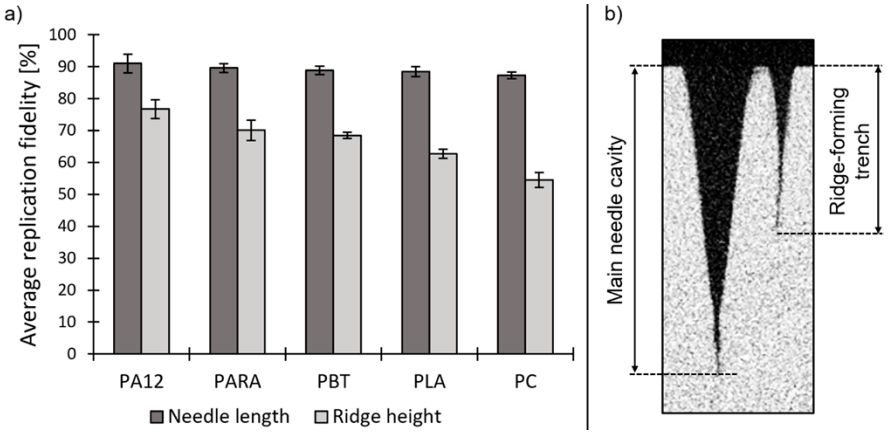

Figure 3. (a) Average replication fidelity of the needle length and ridge height for each of the thermoplastics. (b) Illustration of a micro computed tomography slice of a hollow microneedle cavity.

DOI: https://doi.org/10.51573/Andes.PPS39.GS.IM.4

Difference in Microneedle Replication Fidelity Between the Thermoplastics

Each of the thermoplastics has different material properties, which affects the replication fidelity during injection molding. Using Equation 1, we can estimate the time (t) required for the average temperature of the polymer to reach the no-flow temperature ($T_{no\text{-}flow}$), as shown in [8],

$$t = \frac{a^2}{\pi^2 \cdot \alpha} \cdot ln\left[\frac{8}{\pi^2} \cdot \left(\frac{T_{injection} - T_{mould}}{T_{no-flow} - T_{mould}}\right)\right] \quad 1)$$

with a the thickness of the polymer part, α the thermal diffusivity (calculated using the thermal conductivity, specific heat, and density), $T_{injection}$ the injection temperature, and T_{mould} the mold temperature. Using this equation and the data from Table 1 and Table 2, the time required for PA12, PARA, PBT, PLA, and PC to reach the no-flow temperature are 6.9 s, 5.4 s, 3.6 s, 3.1s, and 1.8 s, respectively. Figure 4 now shows the average replication fidelity of (a) the needle length and (b) the ridge height, along with the time to reach the no-flow temperature for each of the thermoplastics. A clear trend can be observed between the solidification time and the replication fidelity, where a longer solidification time leads to a higher replication fidelity. With a longer solidification time, the polymer melt remains at a higher temperature during the packing phase, ensuring the polymer remains deformable and can continue to fill the microneedle cavity. Conversely, when the solidification time is short, the skin layer of polymer solidifies quickly, preventing further filling of the microneedle cavity.

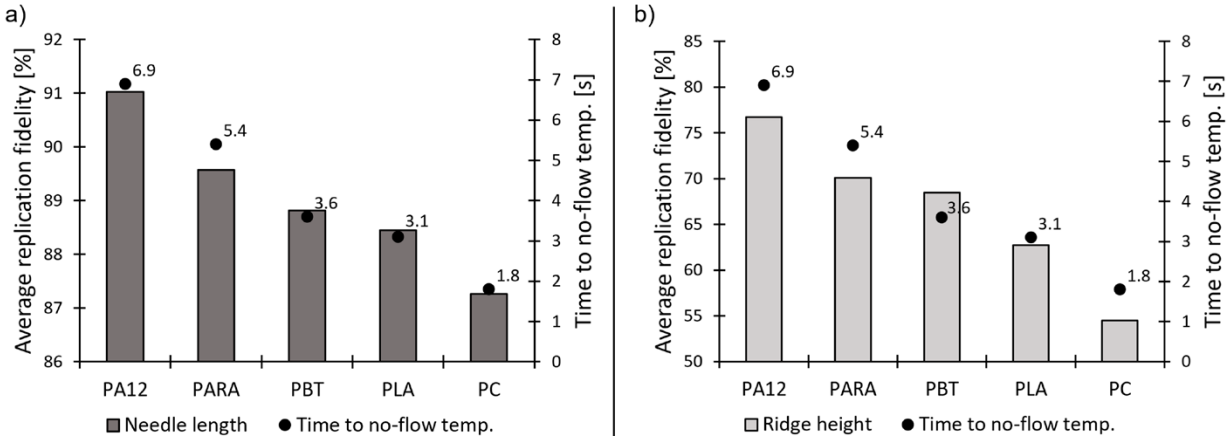

Figure 4. Average replication fidelity of (a) the needle length and (b) the ridge height, together with the time to reach the no-flow temperature for each of the thermoplastics.

DOI: https://doi.org/10.51573/Andes.PPS39.GS.IM.4

Penetration Performance of the Microneedles

Figure 5 shows the force-displacement graphs for penetration tests performed on single microneedles in (a) PA12, (b) PARA, (c) PLA, and (d) PC. In the cases of PA12 (Figure 5[a]) and PLA (Figure 5[c]), no drop in force is observed in the graphs, indicating that there is no penetration event. Microscopic inspection of the microneedles after the penetration tests clearly revealed deformation of the needles, indicating that the needles do not maintain their structural integrity during the penetration test. For PARA (Figure 5[b]), a clear drop in force is consistently observed between 3 to 4 N in every graph. Microscopic inspection of a needle before and after the penetration tests shows no visible deformation. However, it is not possible to determine whether the fibers protruding from the surface were broken or left in the skin after the penetration tests. This issue necessitates further investigation to confirm the integrity and safety of PARA microneedles. For PC (Figure 5[d]), two of the three force-displacement curves show a clear drop in force, occurring between 3.5 to 2.2 N, suggesting that penetration occurs inconsistently. The needle that did not show a drop in force was found to be deformed after the penetration test, indicating an inconsistent performance of PC microneedles.

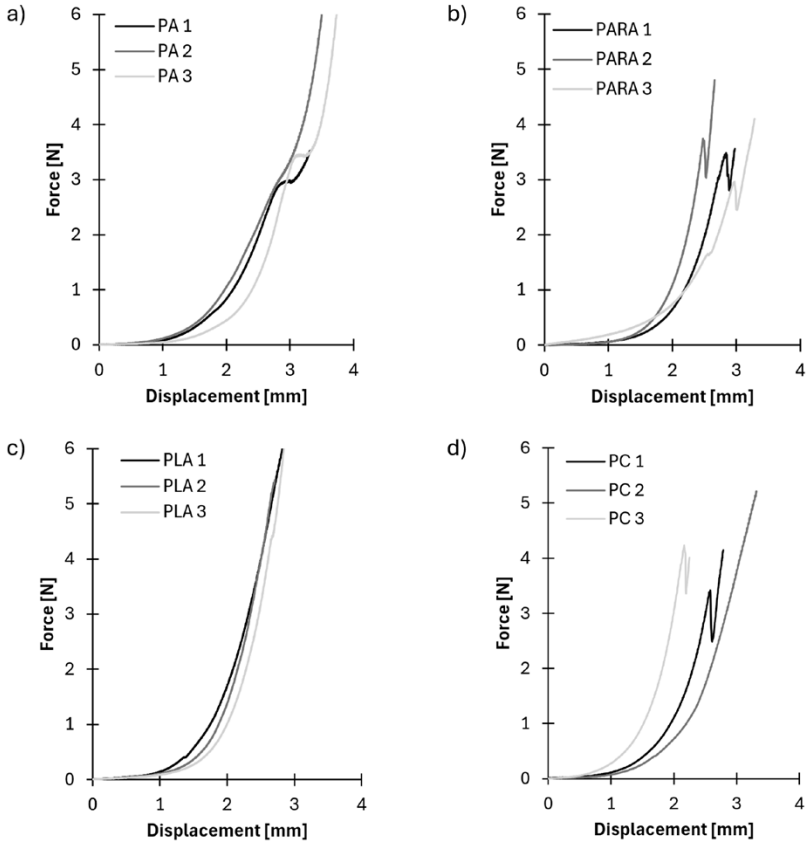

Figure 5. Force-displacement graphs for penetration tests performed on single microneedles in (a) PA12, (b) PARA, (c) PLA, and (d) PC.

DOI: https://doi.org/10.51573/Andes.PPS39.GS.IM.4

A notable trend is observed between the mechanical properties of the thermoplastics, as shown in Table 1, and the penetration success rate. This correlation suggests that achieving consistent and successful penetration requires thermoplastics with higher mechanical properties, particularly the Young's modulus and tensile strength, as seen with PARA.

Conclusion

In this study, we compared five different thermoplastics – PA12, PC, PBT, PLA, and PARA – based on their injection molding characteristics and skin penetration behavior. Significant differences in replication fidelity were observed, influenced by the solidification time of the polymers. Higher solidification times led to better replication fidelity due to extended deformability during the packing phase. Penetration tests revealed that high mechanical properties are essential for successful penetration. PARA exhibited consistent penetration but requires further investigation on the safety of protruding glass fibers. PA12 and PLA microneedles did not penetrate due to the microneedles deforming during the penetration, and PC showed inconsistent performance.

Acknowledgments

This work was funded by the KU Leuven Interdisciplinary Network project IDN/20/011 MIRACLE, as well as the Fonds Wetenschappelijk Onderzoek (FWO)–Vlaanderen SBO S003923N project and SB fellowship 1S31022N. The authors would like to thank Olivier Malek from the company Sirris for laser ablating the microneedle cavities in the mold inserts, and the companies SABIC, Evonik, BioVox, and Syensqo for providing the thermoplastic injection molding materials.

References

1. E. Larrañeta, et al., "Microneedle arrays as transdermal and intradermal drug delivery systems", *Materials Science and Engineering R Reports*, vol. 104, pp. 1–32, 2016.
2. A. Tucak, et al., "Microneedles: Characteristics, materials, production methods and commercial development", *Micromachines*, vol. 11, 2020.
3. T. Evens, et al., "Comparing the Replication Fidelity of Solid Microneedles Using Injection Compression Moulding and Conventional Injection Moulding", *Micromachines*, vol. 13, 2022.
4. T. Evens, et al., "Producing Hollow Polymer Microneedles Using Laser Ablated Molds in an Injection Molding Process", *Journal of Micro and Nano Manufacturing*, vol. 9, pp. 1–9, 2021.
5. P. Vanwersch, et al., "Design, fabrication, and penetration assessment of polymeric hollow microneedles with different geometries", *The International Journal of Advanced Manufacturing Technology*, vol. 132, pp. 533–551, 2024.

6. J.C. Wei, et al., "In vivo, in situ and ex vivo comparison of porcine skin for microprojection array penetration depth, delivery efficiency and elastic modulus assessment", *Journal of the Mechanical Behavior Biomedical Materials*, vol. 130, 2022.

7. T. Evens, et al., "Predicting the replication fidelity of injection molded solid polymer microneedles", *Journal of the Mechanical Behavior of Biomedical Materials*, vol. 37, pp. 237–254, 2022.

8. K.A. Stelson, "Calculating cooling times for polymer injection moulding", *Proceedings of the Institution of Mechanical Engineers, Part B: Journal of Engineering Manufacture*, vol. 217, pp. 709–713, 2003.

DOI: https://doi.org/10.51573/Andes.PPS39.GS.IM.4